Asian Journal of Chemistry; Vol. 28, No. 2 (2016), 277-281

ASIAN JOURNAL OF CHEMISTRY

http://dx.doi.org/10.14233/ajchem.2016.19202

Study on Cobalt Metal Organic Framework Material as Adsorbent for Lead Ions Removal in Aqueous Solution

N.D. SHOOTO[1,*], N. AYAWEI[2], D. WANKASI[1], L. SIKHWIVHILU[3] and E.D. DIKIO[1]

[1]Applied Chemistry and Nano-Science Laboratory, Department of Chemistry, Vaal University of Technology P.O. Box X021, Vanderbijlpark 1900, South Africa
[2]Niger Delta University, Wilberforce Island, P.M.B. 071 Yenagoa Bayelsa State, Nigeria
[3]Advanced Materials Division, Mintek, Nanotechnology Innovation Centre, Private Bag X3015, Randburg 2125, South Africa

*Corresponding author: E-mail: davidshooto12@gmail.com; ezekield@vut.ac.za

Received: 28 March 2015; *Accepted*: 20 July 2015; *Published online*: 3 November 2015; AJC-17590

Cobalt-metal-organic frameworks (Co-MOFs) were synthesized and their morphological features studied using thermalgravimetric analysis, Raman spectroscopy, energy dispersive spectroscopy, scanning electron microscopy, transmission electron microscopy, X-ray diffraction spectroscopy and Fourier transformed infrared spectroscopy. Equilibrium and thermodynamic batch adsorption experiments were carried out to determine concentration, time and temperature effects respectively. The morphological images showed Co-MOFs of irregular sized highly crystalline regions. It also showed the presence of C, O, Co and OH which may create charges and functionalities on the surface of the Co-MOF for adsorption. The adsorption studies recorded a rapid uptake of Pb^{2+} by the Co-MOFs. The equilibrium, kinetic and thermodynamic studies suggested relatively low temperature (low energy) favoured sorption which was exothermic with a physisorption mechanism.

Keywords: Cobalt, Metal-organic frameworks, Solvothermal method, Adsorption.

INTRODUCTION

Heavy metal pollution imposes serious problems to living organisms and the environment. Metals such Pb, Cr and Hg are toxic inorganic pollutants. Ions of these metals even in very low concentration are life threatening. Lead is one of the highly ranked most dangerous heavy metals due to its toxicity [1]. It is widely used in many important industrial applications such as storage battery manufacturing, printing, pigments, fuels, photographic materials and explosives manufacturing [2]. The toxicity of lead to human being is well-known; it replaces calcium and, consequently, can accumulate in the skeletal system. Exposure to lead is associated with a wide range of effects, including various neurodevelopmental effects, mortality (mainly due to cardiovascular diseases), impaired renal function, hypertension, impaired fertility and adverse pregnancy outcomes [3]. This has led to the exploration for adsorbent materials with high affinity for lead ions in aqueous solution. Many materials have been studied as potential lead ion adsorbents; reported materials include polymers like polyvinyl chloride [4], polystyrene and polymethylmethacrylate [5], biomass like coconut shell and palm kernel shell [6] and many more.

Metal-organic frameworks (MOFs) are porous crystalline coordination polymers comprising mono- or multinuclear transition metal centres connected coordinatively through chelating ligands [7,8]. These materials exhibit exceptional unique properties such as high surface area, diversified structures, wide range of pore sizes and are easily functionalized [9-11]. Metal-organic frameworks by their virtue have attracted considerable research interest and are considered as potential candidates for a variety of applications including gas storage, separation, sensing, catalysis, drug delivery, magnetism, *etc.* [12-18]. The synthesis of MOFs can be influenced by many factors such as the nature of metal ions, organic ligands and solvent system. Numerous combinations of metal ions and ligands have resulted in the synthesis of many MOFs with different structures and topologies [19,20].

Several methods have been used in the synthesis of metal-organic frameworks. These methods are (i) direct method and (ii) solvothermal method. In the direct method, metal salt is dissolved in suitable solvent usually in dimethyl formamide at ambient temperature in the presence of triethylamine that initiates reactions and causes deprotonation of the organic linker to precipitate the MOF crystals [21]. The solvothermal method can be performed by heating a mixture of metal salt

and organic linker in a solvent system that containing dimethyl formamide [22]. In this study cobalt metal organic framework (Co-MOF) is synthesized by reacting cobalt(II) nitrate and 1,2,4,5-tetrabenzene carboxylic acid, characterized and employed as adsorbent for the removal of lead ions in aqueous solutions.

EXPERIMENTAL

N,N-Dimethylformamide (DMF, 99.8 %; AnalaR), cobalt(II)nitrate hexahydrate (98 %, Sigma-Aldrich), 1,2,4,5-tetrabenzenecarboxylic acid (96 %, Sigma-Aldrich), methanol (99.9 %; Sigma-Aldrich) and lead nitrate. All the reagents were obtained from commercial sources and used without further purification.

Co-MOF by solvothermal method: $Co(NO_3)_2$ (0.012 mol) and 1,2,4,5-tetrabenzene carboxylic acid (0.012 mol) were dissolved in 80 mL DMF by mild stirring. The solution was then transferred to a round bottom flask and refluxed for 2 h at 120 °C while stirring. Pink crystalline powder was obtained. After centrifugation the product was collected and washed several times with methanol to remove excess DMF molecules. Sample was dried in the oven set to 40 °C for 0.5 h.

Characterization: The chemical features of the as-prepared Co-MOF were analyzed by SEM, EDS, XRD, FTIR, TGA and Raman spectra. The surface morphology and EDS measurements were recorded with a JOEL 7500F Emission scanning electron microscope. X-ray diffractometer (XRD), Shimadzu XRD 7000 was used to identify obtained sample. Thermogravimetric Analyzer (TGA), Perkin Elmer TGA 4000 was used, analyses were performed from 30 to 900 °C at a heating rate of 10 °C/min under a nitrogen atmosphere. Fourier transformed infrared spectroscopy (FTIR), Perkin Elmer FT-IR/FT-NIR spectrometer, spectrum 400. The measuring range extended from 4000 to 520 cm^{-1}. Raman spectra were acquired using a PerkinElmer Raman Station 400 benchtop Raman spectrometer. The excitation source was a near-infrared 785 nm laser (100 mW at the sample), with a spot size 100 μm. A spectra range of 3200-100 cm^{-1} was employed

Lead solution preparation: The stock solution of Pb^{2+} (100 mg/L) was prepared by dissolving 0.1 g $Pb(NO_3)_2$ in 1 L of distilled water. Dilutions were made to 80, 60, 40 and 20 mg/L, respectively.

Batch adsorption experiment: Batch adsorption experiments were carried out to determine concentration and temperature effects and time dependent studies. 0.05 g of the as-prepared Co-MOF and initial Pb^{2+} ion concentrations of 20, 40, 60, 80 and 100 mg/L were used for the concentration effect. For the temperature effect, the same weight of polymer sample was used with time intervals of 5, 10, 15, 20, 40 and 60 min. The values of 25, 40, 60 and 80 °C were used with the same weight of polymer to study the temperature effect. Standard methods of the batch equilibrium studies were applied for the concentration, temperature and time dependent experiments.

Data analysis: Various equilibrium, kinetic and thermodynamic models (equations) were employed to interpret the data and establish the extent of adsorption. The amount of metal uptake was computed using the material balance equation for batch dynamic studies (eqn. 1)

$$q_e = \frac{V}{M}(C_o - C_e) \quad (1)$$

The essential characteristics of the Langmuir isotherm were expressed in terms of a dimensionless separation factor or equilibrium parameter S_f. Where C_o is initial concentration of Pb^{2+} in solution. If $S_f > 1.0$, the isotherm is unfavourable; $S_f = 1.0$ (linear), $0 < S_f < 1.0$ (favourable) and $S_f = 0$ (irreversible) (eqn. 2):

$$S_f = \frac{1}{1 + aC_o} \quad (2)$$

The fraction of MOF surface covered by Pb^{2+} was computed using with θ as degree of surface coverage (eqn. 3):

$$\theta = 1 - \frac{C_e}{C_o} \quad (3)$$

The effectiveness of the adsorbent (Co-MOF) was assessed by the number of cycles of equilibrium sorption process required to reduce the levels of Pb^{2+} in solution according to the value of the distribution (partition coefficient (K_d)) in where C_{aq} is concentration of Pb^{2+} in solution, mg/L; C_{ads} is concentration of Pb^{2+} in MOF in mg/L (eqn. 4)

$$K_d = \frac{C_{ads}}{C_{aq}} \quad (4)$$

The removal efficiency of an adsorbent in an adsorption system is expressed eqn. 5 where R_E is the removal efficiency (%), C_o is the initial concentration of adsorbate mg/L and C_e is the equilibrium concentration of adsorbate in mg/mL

$$R_E = \left(\frac{C_o - C_e}{C_o}\right) \times 100 \quad (5)$$

RESULTS AND DISCUSSION

To determine the morphology and examine the crystal size of the as-prepared Co-MOF, scanning electron microscope image was taken at micro-scale. The SEM image shows irregular sized crystals, as shown in Fig. 1. The most fascinating characteristic advantage of MOFs is their exceptionally high surface area [23]. Large surface area of any adsorbent facilitates maximum adsorption

Energy dispersive spectroscopy (EDS) was employed for elemental analysis of the as-prepared Co-MOF sample. The EDS spectrum in Fig. 2 showed multiple peaks due to the following elements: C (78.4 %), O (18.4 %) and Co (3.3 %) as presented in Table-1. The presence of these elements will create charges on the surface of the as-prepared Co-MOF and result in electrostatic forces between the sample and Pb^{2+} in the solution.

Weight loss profile from thermogravimetric analysis (TGA) and derivative thermogravimetric analysis (DTGA) are presented in Fig. 3. The TGA and DTGA profiles show multiple stages in weight loss. First decomposition was observed from 35-120 °C, this could be due to loss of absorbed moisture and water molecules present and washing (methanol) removal from the cavities. A continuous mass loss from 200-500 °C was observed in the plot, this mass loss probably corresponds to

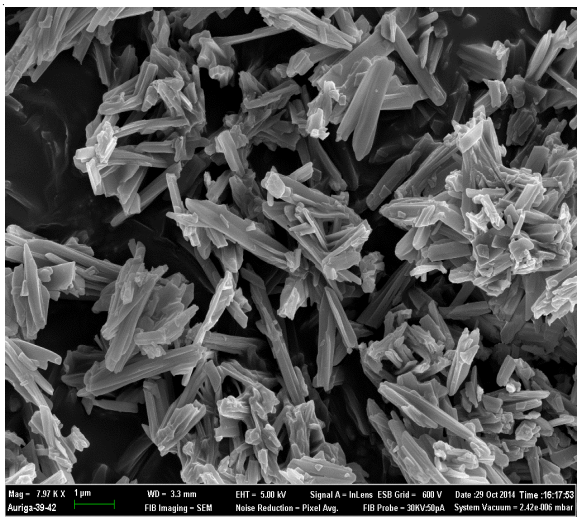

Fig. 1. Scanning electron micrograph image of synthesized cobalt metal organic framework obtained from cobalt(II) nitrate reacted with 1,2,4,5-tetrabenzene carboxylic acid

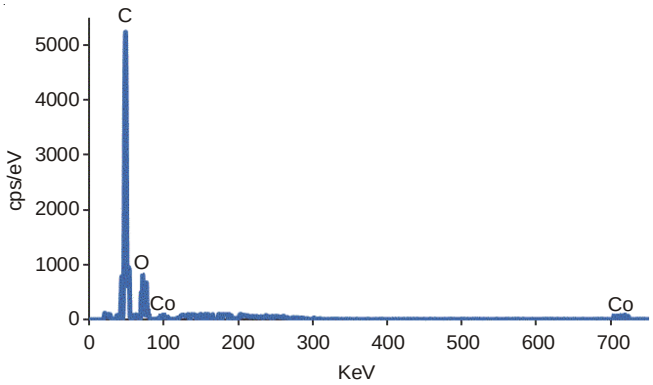

Fig. 2. Energy dispersive spectroscopy (EDS) of synthesized cobalt metal organic framework obtained from cobalt(II) nitrate reacted with 1,2,4,5-tetrabenzene carboxylic acid

TABLE-1
WEIGHT (%) OF ELEMENT AND ATOM OBTAINED FROM ENERGY DISPERSIVE SPECTROSCOPY OF COBALT METAL ORGANIC FRAMEWORK

Element	Atom (%)	Peak height (a.u)
Carbon	78.4	5227
Oxygen	18.4	822
Cobalt	3.3	92
Total	100	100

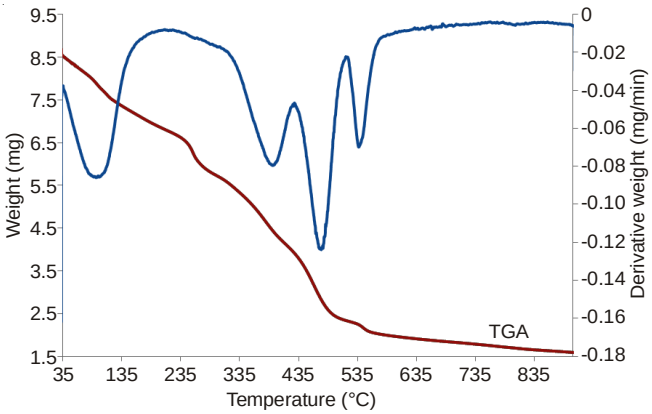

Fig. 3. Thermogravimetric analysis and derivative thermogravimetric analysis of cobalt metal organic framework

the removal of all organic material, including the evaporation of guest molecules from the pores such as DMF. Between 510-550 °C the weight loss was observed indicating the decomposition of organic ligands on the MOF

The crystal structure of the prepared Co-MOFs was characterized by the X-ray diffraction. As shown in Fig. 4, the diffraction peaks of the Co-MOF were consistent with the theoretical patterns from the single crystal data and with those previously reported in the literature [24]. Very sharp peak below 10° at 8.6 was observed on the diffractogram indicating that highly crystalline materials were synthesized [25].

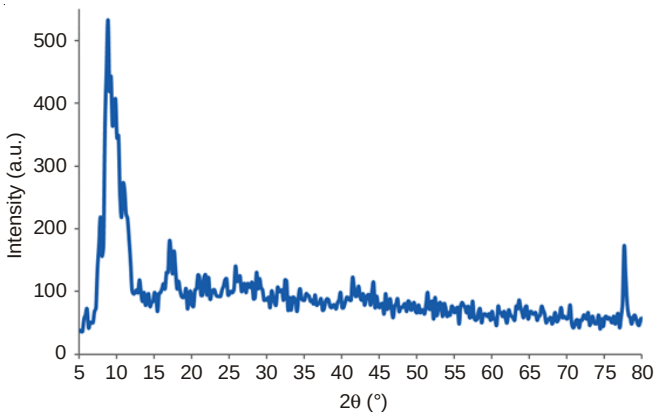

Fig. 4. X-ray diffraction spectra of synthesized cobalt metal organic framework

The FT-IR spectrum is presented in Fig. 5. The broad peak located at 3414 cm^{-1} is assigned to the O-H vibration from the intermolecular and intramolecular hydrogen bonds. Two vibration bands at 1581 and 1384 cm^{-1} refers to the stretching C-H from alkyl groups and the peaks at 1704 and 1660 cm^{-1} correspond to the symmetric and asymmetric stretching C=O and C-O in carboxylic respectively. The vibration bands at 1143-790 cm^{-1} can be attributed to the fingerprint of 1,2,4,5-tetrabenzene carboxylic acid compounds. The peak found at 683 cm^{-1} is related to the Co-O stretching vibration.

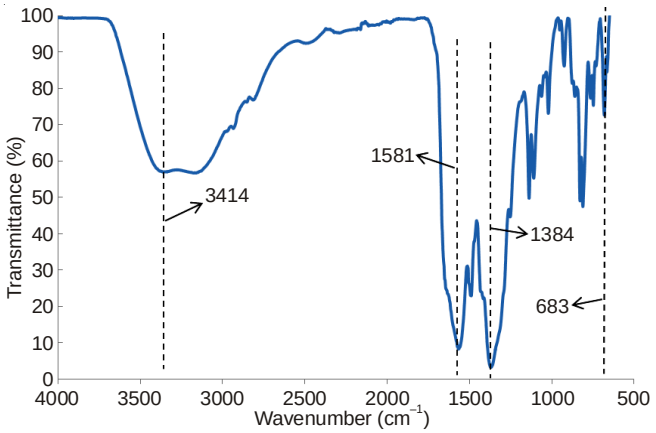

Fig. 5 Fourier transform infrared spectra of synthesized cobalt metal organic framework

Raman spectra were recorded for Co-MOFs samples (Fig. 6). Multiple Raman bands were observed at 1606, 1444, 1190, 648, 406 cm^{-1}. These bands are associated with vibration modes of aromatic breathing and vibration modes of carboxylate symmetric stretch.

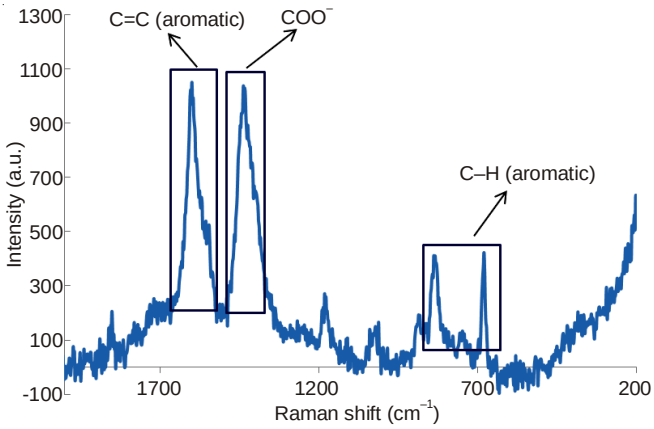

Fig. 6. Raman spectra of synthesized cobalt metal organic framework

The percentage adsorption of Pb^{2+} by the Co-MOF at different concentrations of the Pb^{2+} is presented in Fig. 7. At lower concentration more Co-MOF pore spaces were available for the Pb^{2+}, but equilibrium was not attained because the adsorption took place in multilayers. The results indicated that the sorption of Pb^{2+} were very much dependent on the concentration of the Pb^{2+}.

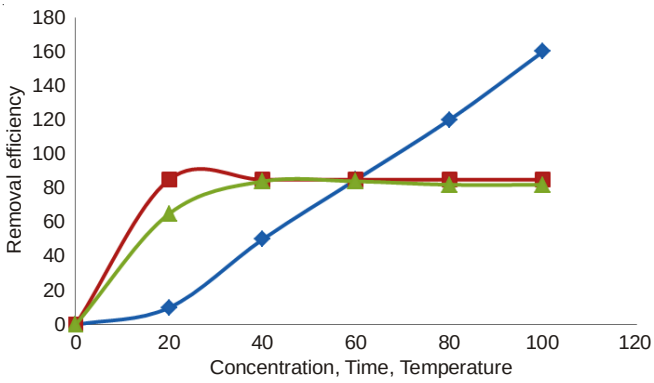

Fig. 7. Adsorption efficiency of Co-MOF with Pb^{2+} at (a) - ◆ - concentration (mg/L), (b) - ■ - Time (min) and (c) - ▲ - Temperature (°C)

Time dependency studies show the amount of time needed for maximum adsorption to occur. The variation in percentage removal of Pb^{2+} with time has been presented in Fig. 7. It indicates that a maximum of 85 % removal of Pb^{2+} was observed in 20 min and remained constant afterwards. The relatively short contact time required to attain equilibrium suggests that a rapid uptake of Pb^{2+} by the Co-MOF occurred to fill some of the vacant pores in the carbon nanotube and after which the remaining spaces were difficult to be occupied due to repulsive forces between the Pb ions.

Fig. 7 also presents the plot of percentage adsorption of Pb^{2+} by the Co-MOF at varying temperatures with optimum sorption of 85 % occurring at 28 °C. The plot showed that further increase in temperature resulted in no significant increase in adsorption. This may be attributed to the presence of both physical and chemical adsorption with chemisorption predominating.

The effectiveness of the Co-MOF as an adsorbent for Pb^{2+} from solution was assessed through the sorption distribution or partition coefficient K_d presented in Table-2. The value of K_d (0.214) suggests that the Co-MOF is an effective adsorbent,

TABLE-2
EQUILIBRIUM AND KINETIC PARAMETERS

Surface coverage (θ)	0.7860
Separation factor (S_f)	0.2936
Sorption coeffienct (K_d)	0.2140
Adsorption capacity (mol/g)	85.72
Removal efficiency (%)	71.9

but more number of cycles of equilibrium sorption process will be required to reduce the levels of Pb^{2+} in solution.

In order to determine the nature of the adsorption process, whether favourable or unfavourable, the dimensionless constant separation term S_f was investigated (eqn. 2). The result (S_f = 0.294) in Table-2 was less than one and greater than zero which showed that the sorption of Pb^{2+} onto the Co-MOF was favourable.

The fraction of the Co-MOF surface covered by the Pb^{2+} is given as 0.79 (Table-2). This value indicates that 79 % of the pore spaces of the Co-MOF surface were covered by Pb^{2+}, which means high degree of adsorption.

Conclusion

Cobalt-metal-organic frameworks were successfully synthesized and the results of the characterization confirmed irregular sized highly crystalline materials. The equilibrium and kinetic batch adsorption studies recorded rapid and effective uptake of the Pb^{2+} by the Co-MOF as shown in the results. The adsorption was favoured at low temperature and energy which was exothermic with a both physico-sorption and chemisorption mechanisms. The results from this study will add to the knowledge base on the synthesis, characterization and the use of metal organic frameworks for the sorption studies.

ACKNOWLEDGEMENTS

This work was supported by a research grant from Faculty of Applied and Computer Science Research and Publications Committee of Vaal University of Technology. Mintek is gratefully acknowledged for permitting to use their equipments.

REFERENCES

1. A. Azizullah, M.N.K. Khattak, P. Richter and D.H. Hader, *Environ. Int.*, **37**, 479 (2011).
2. R. Jalali, H. Ghafourian, Y. Asef, S.J. Davarpanah and S. Sepehr, *J. Hazard. Mater.*, **92**, 253 (2002).
3. R.P. Suresh Jeyakumar and V. Chandrasekaran, *Int. J. Ind. Chem.*, **5**, 2 (2014).
4. D. Wankasi and E.D. Dikio, *J. Chem.*, Article ID 817527 (2014).
5. D. Wankasi and E.D. Dikio, *Asian J. Chem.*, **24**, 8295 (2014).
6. D. Wankasi and E.D. Dikio, *Asian J. Chem.*, **27**, 690 (2015).
7. R. Banerjee, H. Furukawa, D. Britt, C. Knobler, M. O'Keeffe and O.M. Yaghi, *J. Am. Chem. Soc.*, **131**, 3875 (2009).
8. H.K. Chae, D.Y. Siberio-Perez, J. Kim, Y. Go, M. Eddaoudi, A.J. Matzger, M. O'Keeffe and O.M. Yaghi, *Nature*, **427**, 523 (2004).
9. M. Eddaoudi, J. Kim, N. Rosi, D. Vodak, J. Wachter, M. O'Keeffe and O.M. Yaghi, *Science*, **295**, 469 (2002).
10. G. Ferey, *Chem. Soc. Rev.*, **37**, 191 (2008).
11. G. Ferey, C. Mellot-Draznieks, C. Serre, F. Millange, J. Dutour, S. Surble and I. Margiolaki, *Science*, **309**, 2040 (2005).
12. P. Horcajada, R. Gref, T. Baati, P.K. Allan, G. Maurin, P. Couvreur, G. Ferey, R.E. Morris and C. Serre, *Chem. Rev.*, **112**, 1232 (2012).
13. C. Lamberti, A. Zecchina, E. Groppo and S. Bordiga, *Chem. Soc. Rev.*, **39**, 4951 (2010).
14. K. Sumida, D.L. Rogow, J.A. Mason, T.M. McDonald, E.D. Bloch, Z.R. Herm, T.H. Bae and J.R. Long, *Chem. Rev.*, **112**, 724 (2012).

15. M.P. Suh, H.J. Park, T.K. Prasad and D.W. Lim, *Chem. Rev.*, **112**, 782 (2012).
16. D. Maspoch, D. Ruiz-Molina, K. Wurst, N. Domingo, M. Cavallini, F. Biscarini, J. Tejada, C. Rovira and J. Veciana, *Nat. Mater.*, **2**, 190 (2003).
17. M. Kawano, T. Kawamichi, T. Haneda, T. Kojima and M. Fujita, *J. Am. Chem. Soc.*, **129**, 15418 (2007).
18. G. Férey, F. Millange, M. Morcrette, C. Serre, M.L. Doublet, J.M. Grenèche and J.M. Tarascon, *Angew. Chem Int. Ed. Engl.*, **46**, 3259 (2007).
19. P.D.C. Dietzel, V. Besikiotis and R. Blom, *J. Mater. Chem.*, **19**, 7362 (2009).
20. K.K. Tanabe and S.M. Cohen, *Inorg. Chem.*, **49**, 6766 (2010).
21. D.J. Tranchemontagne, J.R. Hunt and O.M. Yaghi, *Tetrahedron*, **64**, 8553 (2008).
22. C.S. Tsao, M.S. Yu, C.Y. Wang, P.Y. Liao, H.L. Chen, U.S. Jeng, Y.R. Tzeng, T.Y. Chung and H.C. Wu, *J. Am. Chem. Soc.*, **131**, 1404 (2009).
23. H. Wang, F. Yin, G. Li, B. Chen and Z. Wang, *Int. J. Hydrogen Energy*, **39**, 16179 (2014).
24. H.-Y. Cho, D.-A. Yang, J. Kim, S.-Y. Jeong and W.-S. Ahn, *Catal. Today*, **185**, 35 (2012).
25. R.A. Crowther, D.J. Derosier and A. Klug, *Proc. R. Soc. Lond. A Math. Phys. Sci.*, **319**, 40 (1970).